PUB-78-116-E
E-104

E4

UM HE 78-2
20 March 1978

Neutron-Proton Elastic Scattering from 70 to 400 GeV/c*

C.E. DeHaven Jr., C.A. Ayre†, H.R. Gustafson, L.W. Jones,
M.J. Longo, P.V. Ramana Murthy§, T.J. Roberts, M.R. Whalley

Randall Laboratory of Physics
University of Michigan
Ann Arbor MI 48109

ABSTRACT

We have measured neutron-proton elastic scattering cross sections for four-momentum transfers $.17 \leq -t \leq 3.5 (\text{GeV/c})^2$. The logarithmic slope parameter is found to be consistent with existing proton-proton parameterizations. The data also exhibit a dip in the cross section near $-t \approx 1.4 (\text{GeV/c})^2$ for incident neutron momenta above 200 GeV/c. Differences between n-p and p-p cross sections are noted in the region $.7 \leq -t \leq 1.4 (\text{GeV/c})^2$.

We report results of an experiment at Fermi National Accelerator Laboratory to measure neutron-proton elastic scattering using techniques developed in previous experiments.[1,2] These measurements were made with an incident neutron beam which had a continuous spectrum extending to 400 GeV/c. Four-momentum transfers from $.17(\mathrm{GeV/c})^2$ to $\sim 3.5(\mathrm{GeV/c})^2$ were covered with particular attention being paid to the region $-t \approx 1.4(\mathrm{GeV/c})^2$ where structure has been previously reported[3-5] in p-p elastic scattering.

A schematic diagram of the experiment is shown in Figure 1. The neutron beam was incident upon a liquid hydrogen target, 30.5 cm long and 5.1 cm diameter. The recoil proton momentum and scattering angle were measured by a spectrometer consisting of four wire spark chamber modules each with X-Y-U-V magnetostrictive readout planes, and a 105 cm x 100 cm analyzing magnet with a 15.1 cm gap. Part of the trigger requirement was a fast coincidence between scintillation counters P_1, P_2, and P_3 which indicated that a charged particle had traversed the spectrometer. The scattered neutron was detected by requiring it to interact in a neutral particle detector and produce a charged particle shower. The detector contained 30 wire spark chambers, 28 zinc plates and six scintillation counters (see inset of Fig. 1) and was placed 71 m downstream of the hydrogen target. The interaction point was determined to an accuracy $\sim$2 mm FWHM by locating the vertex of the charged particle shower in the chambers. The neutron scattering angle was then found by connecting the interaction point in the neutral particle detector with a point in the liquid hydrogen target on the proton trajectory. The second part of the triggering requirement was a fast coincidence between any two of the six scintillation counters indicating that at least one charged particle had passed through the detector. Veto counters $A_1 \ldots A_6$, not all of which are shown in Figure 1, were used to reduce the trigger rate from inelastic events. A counter telescope M and a total absorption calorimeter were used to monitor the beam flux.

All kinematic variables were measured except for the momenta of the incident and scattered neutrons. Thus momentum and energy conservation allowed a two-constraint fit to the hypothesis of n-p elastic scattering. The fitting program calculated the unmeasured momenta and a χ^2 for the fit. Events with $\chi^2 < 10$ were considered to be elastic and were binned according to the incident neutron momentum and the four-momentum transfer squared, t.

Various corrections have been applied to the data. The geometric acceptance was calculated using Monte Carlo methods. Inelastic background corrections, as estimated from χ^2 distributions, amounted to less than 3% at small $|t|$ and less than 35% at large $|t|$. Corrections for nuclear absorption of the recoil proton ranged from 2 to 4%. Target empty corrections were negligible. It is important to note that the neutron detection efficiency, which was about 65%, does not significantly affect the t-dependence of the measured cross sections because the energy of the scattered neutron differs from that of the incident neutron by at most 2%.

The resolution in t is independent of the incident neutron momentum and is determined by multiple Coulomb scattering of the recoil proton and the resolution of the proton spectrometer. The uncertainty in t was less than 1% at $|t| = 1.5$ $(\mathrm{GeV/c})^2$. The resolution of the incident neutron momentum p is t-dependent since the neutron scattering angle is correlated with the recoil proton scattering angle. At 200 GeV/c and $|t| = 1.4$, the uncertainty in momentum was less than 6 GeV/c.

Four settings of the apparatus were used. Relative normalization between settings was accomplished by tying the data together smoothly in various overlap regions. After the data were combined, the overall normalization was calculated by fitting the data to the form $d\sigma/d|t| = Ae^{Bt+Ct^2}$ in the range $.17 \leq |t| \leq .7$ and extrapolating to $t = 0$. The intercept was then adjusted to the optical theorem point as given by

$$\frac{d\sigma(t=0)}{d|t|} = \frac{1}{16\pi}\,\sigma_T^2\,(1+\rho^2). \qquad (1)$$

The values of σ_T used were calculated from a fit of n-p total cross section data given by Murthy et al.[6] If we assume that the ratio of the real to imaginary parts of the forward scattering amplitude, ρ, for n-p elastic scattering is approximately the same as that for p-p scattering,[7] the contribution of the ρ^2 term in Eq. 1 is negligible. The uncertainty in the overall normalization is estimated to be $^{+5}_{-15}\%$, mainly due to the uncertainty in the extrapolation to t=0.

A total of 1.1×10^6 triggers were recorded; of these 2.7×10^5 were considered elastic events. The data are presented in Figure 2 for seven incident momentum bins. The errors shown include the statistical and the correction factor uncertainties but not the scale factor uncertainty. The incident momentum attached to each graph is that of the bin center.

The data exhibit the usual diffraction peak which shrinks with increasing energy. Using the fit Eq. 1, we have evaluated the logarithmic slope at $-t = .2(\mathrm{GeV/c})^2$. The results are shown in Figure 3 along with previous measurements for n-p[8,9] and p-p[10,11] elastic scattering. The slope parameters have been plotted as a function of s, the center-of-mass energy squared. Our slopes agree with corresponding p-p data and also with the Reggeized global absorption model of Kane and Seidl.[12]

The data also show the gradual evolution of a dip in the cross section near $-t \approx 1.4(\mathrm{GeV/c})^2$ as the incident neutron energy increases. While the dip is similar to that observed in p-p data, we find the n-p cross sections are generally higher in this region.

We have compared our data with existing p-p elastic scattering data from Fermilab[3,4] at 100 and 200 GeV/c. At the lower momentum, the cross sections are comparable out to

$-t \approx 0.8(\text{GeV/c})^2$. At larger t, they begin to diverge with the n-p cross section approximately 3 times the p-p cross section near $-t \approx 1.25$. This difference extends to $-t \approx 1.4(\text{GeV/c})^2$. A comparison of the 200 GeV/c p-p data with the 175-225 GeV/c n-p data in the region $.7<-t<1.5$ is shown in Figure 4. In this momentum range, the cross sections for n-p and p-p remain comparable out to $-t \approx .95(\text{GeV/c})^2$, beyond which they begin to diverge. As in the 100 GeV/c data, the n-p cross section is 3 times the p-p data near $-t \approx 1.25(\text{GeV/c})^2$. In order to see if the n-p data exhibit a strong energy dependence we have also binned the data for the incident momentum range 200 to 240 GeV/c as shown in Figure 4. The cross sections remain unchanged out to $-t \approx 1.3(\text{GeV/c})^2$.

Also in Figure 4, our 280 GeV/c data is compared to ISR data[5] at a lab equivalent energy of 282 GeV/c. We find the n-p and p-p cross sections are in good agreement out to $-t \approx 1.2(\text{GeV/c})^2$. In a Regge model, the difference between n-p and p-p elastic scattering is caused by a change in the sign of the ρ and A_2 isovector exchange amplitudes. The magnitude of these amplitudes should decrease with increasing energy. Our results indicate just such an effect. As s increases, the n-p and p-p cross sections are comparable out to larger values of t. By 280 GeV/c, the contribution of the ρ and A_2 would seem to be quite small. The fact that the n-p cross sections are greater indicates that net helicity flip amplitudes may be important in this region.

We wish to express our appreciation to the entire Fermilab staff for their support of this experiment. We also wish to thank Jim Stone, John Chanowski, Geoff Mills and Bill Larsen for their help during various phases of the experiment. Useful discussions with Gordon Kane and Andy Seidl are gratefully acknowledged.

*Work supported by the National Science Foundation

†Present Address: Department of Physics, University of Durham, Durham, England

§Permanent Address: Tata Institute for Fundamental Research, Bombay, India

REFERENCES

1. J.L. Stone et al., Phys. Rev. Lett. 38, 1315 (1977).
2. M.L. Perl et al., Phys. Rev. D1, 1857 (1970).
3. C.W. Akerlof et al., Phys. Lett. 59B, 197 (1975).
4. R. Bomberowitz, Ph.D. Thesis, Rutgers University (Physics) 1977; R. Bomberowitz et al., Bull. Am. Phys. Soc. 23, 52 (1978).
5. N. Kwak et al., Phys. Lett. 58B, 233 (1975).
6. P.V.R. Murthy et al., Nucl. Phys. B92, 269 (1975).
7. V. Bartenev et al., Phys. Rev. Lett. 31, 1367 (1973).
8. V. Böhmer et al., Nucl. Phys. B91, 266 (1975).
9. J.L. Stone et al., University of Michigan Report No. UM HE 77-46 (submitted to Nucl. Phys. B).
10. G. Barbiellini et al., Phys. Lett. 39B, 663 (1972).
11. D.S. Ayres et al., Phys. Rev. Lett. 35, 1195 (1975).
12. G. L. Kane and A. Seidl, Rev. Mod. Phys. 48, 309 (1976).

FIGURE CAPTIONS

Figure 1. Schematic layout of the experimental apparatus. The inset shows the neutron detector in more detail.

Figure 2. Neutron-proton differential cross sections in $mb/(GeV/c)^2$ for seven incident momentum bins. The momenta indicated are the center of the bins.

Figure 3. Logarithmic slope parameter plotted as a function of the center-of-mass energy squared s for n-p and p-p elastic scattering. The solid curve is a prediction from Kane and Seidl.[12]

Figure 4. Neutron-proton cross sections in $mb/(GeV/c)^2$ for 175-225 GeV/c, 200-240 GeV/c (only four data points are shown) and 265-300 GeV/c bins. Also shown are the results of Akerlof et al.[3] and preliminary data from Bomberowitz et al.[4] for proton-proton elastic scattering at 200 GeV/c.

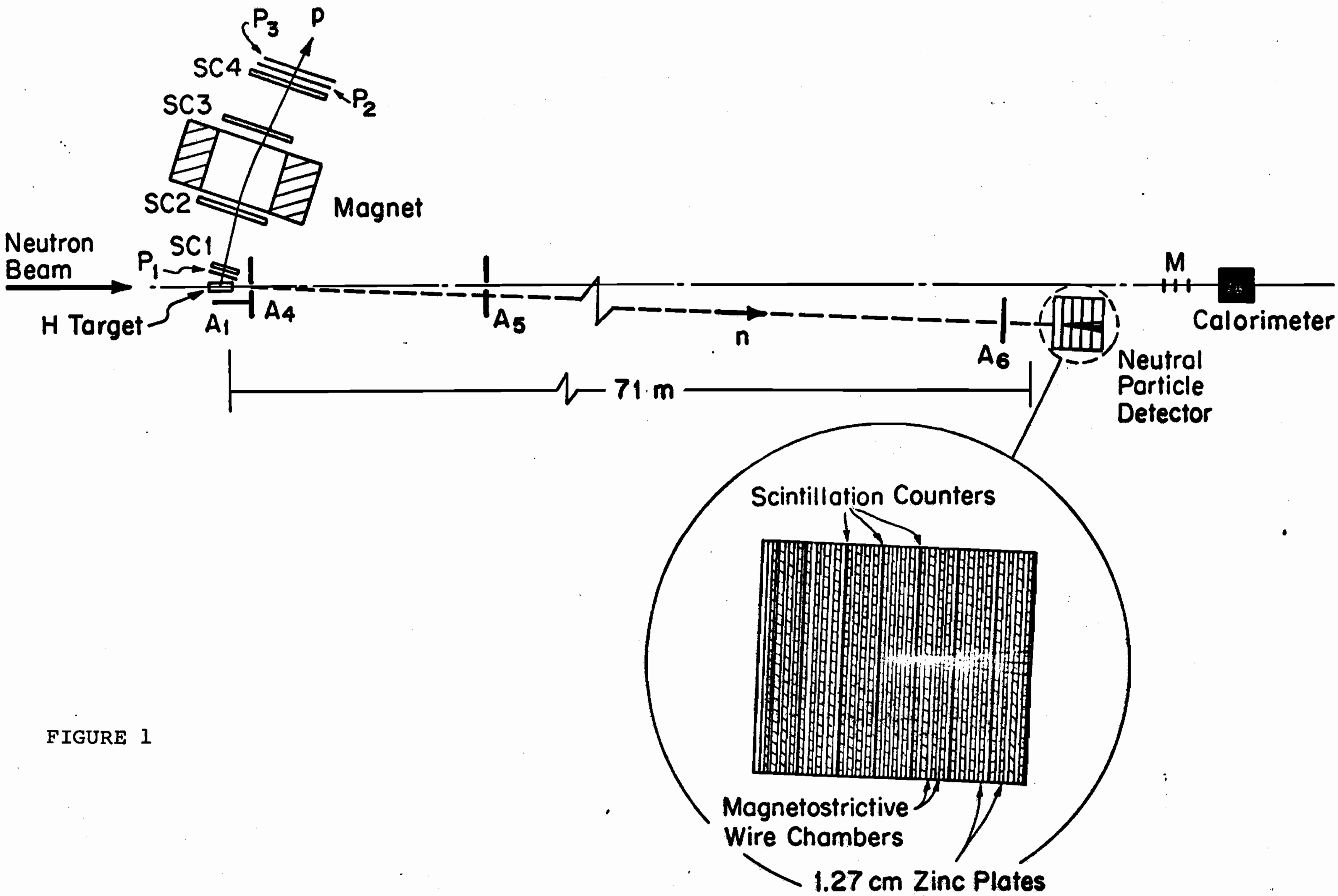

P3
p
SC4
P2
SC3
SC2
Magnet
Neutron
Beam
SC1
P1
H Target
A1
A4
A5
n
M
Calorimeter
A6
Neutral
Particle
Detector
71 m
Scintillation Counters
Magnetostrictive
Wire Chambers
1.27 cm Zinc Plates

FIGURE 1

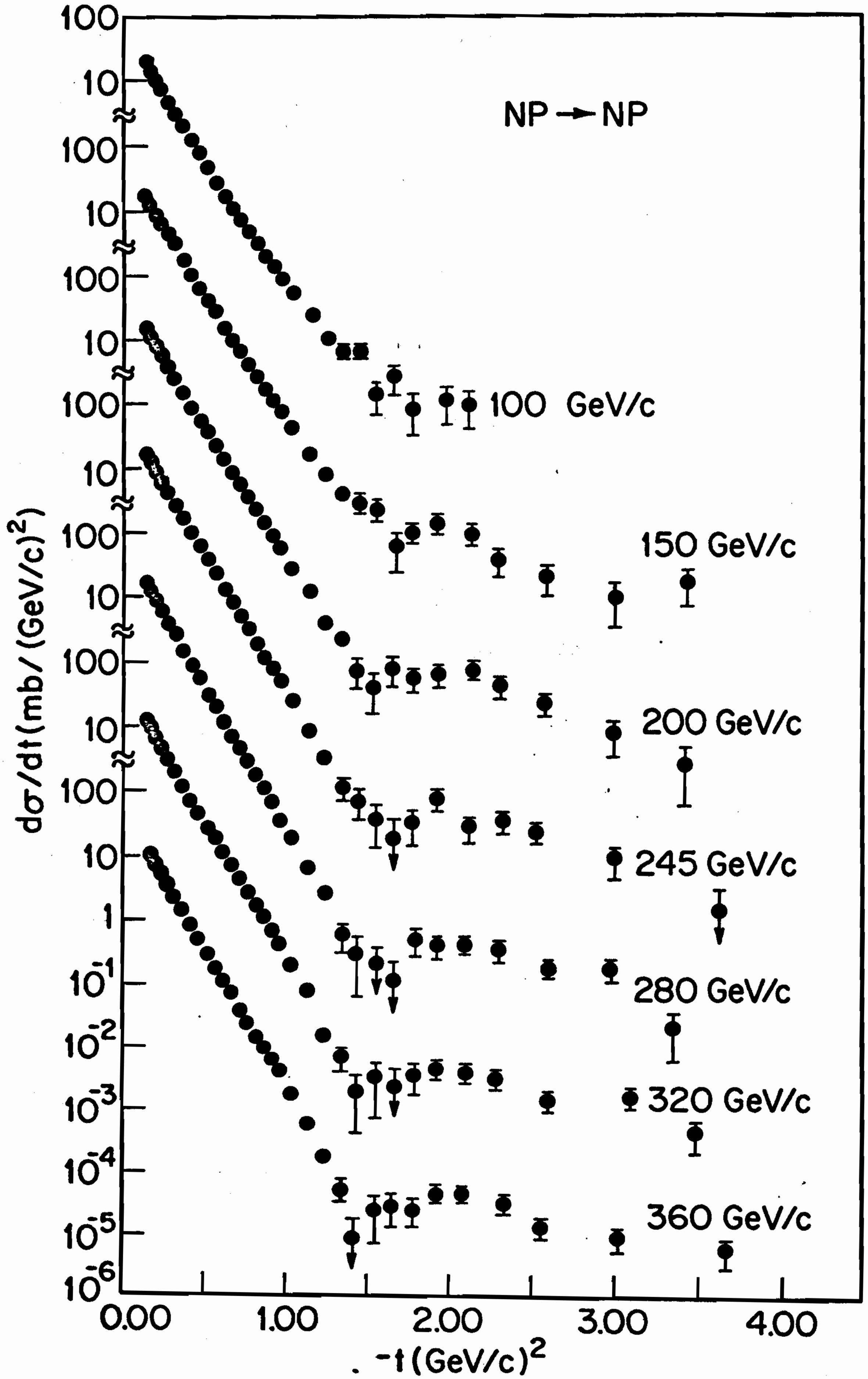
NP → NP
100 GeV/c
150 GeV/c
200 GeV/c
245 GeV/c
280 GeV/c
320 GeV/c
360 GeV/c
dσ/dt(mb/(GeV/c)²)
-t (GeV/c)²
0.00
1.00
2.00
3.00
4.00

FIGURE 2

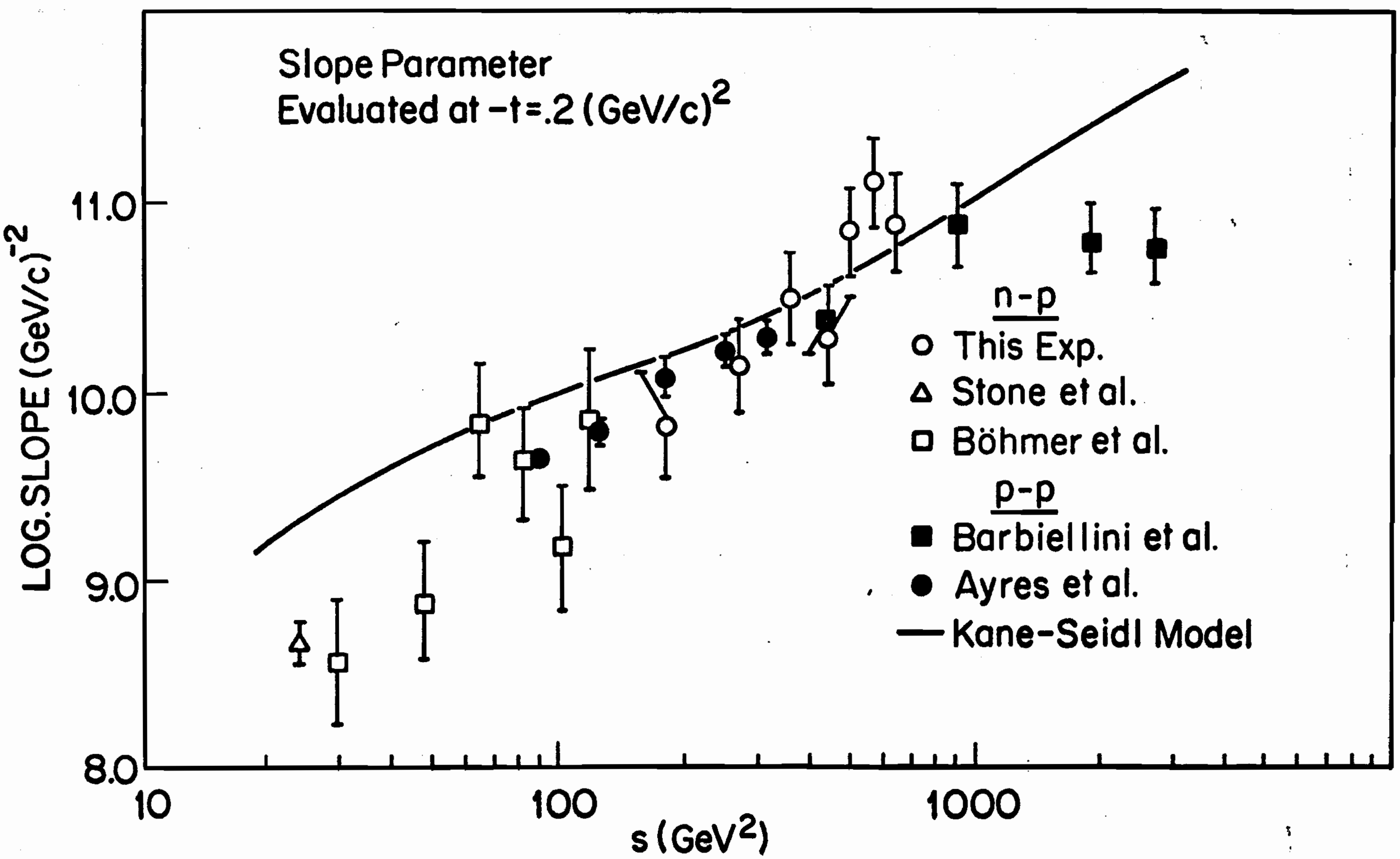
Slope Parameter
Evaluated at −t=.2 (GeV/c)²
LOG. SLOPE (GeV/c)⁻²
11.0
10.0
9.0
8.0
10
100
1000
s (GeV²)
n-p
This Exp.
Stone et al.
Böhmer et al.
p-p
Barbiellini et al.
Ayres et al.
Kane-Seidl Model

FIGURE 3

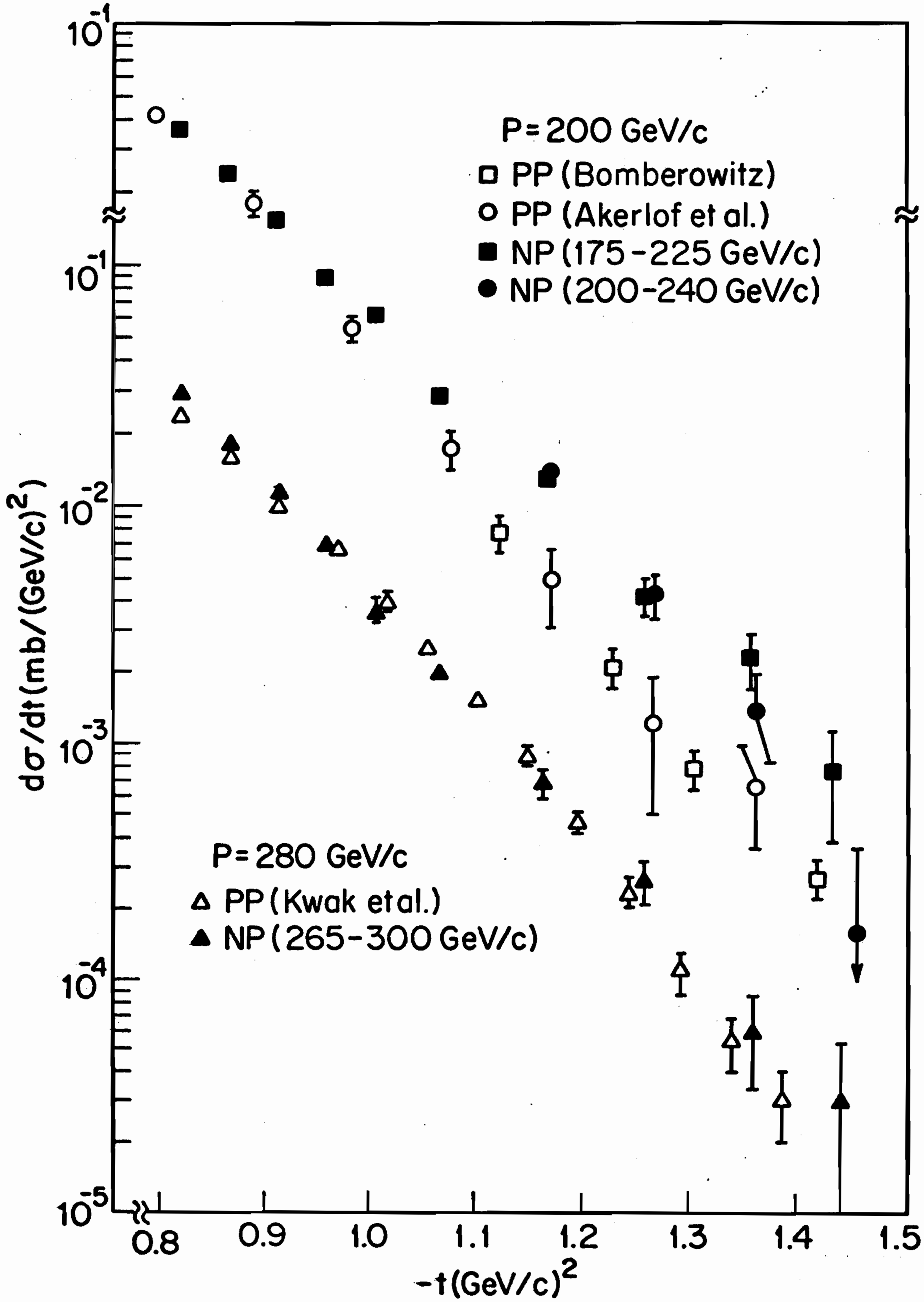

P= 200 GeV/c
PP (Bomberowitz)
PP (Akerlof et al.)
NP (175-225 GeV/c)
NP (200-240 GeV/c)
P= 280 GeV/c
PP (Kwak et al.)
NP (265-300 GeV/c)
dσ/dt (mb/(GeV/c)²)
-t (GeV/c)²
10⁻¹
10⁻¹
10⁻²
10⁻³
10⁻⁴
10⁻⁵
0.8
0.9
1.0
1.1
1.2
1.3
1.4
1.5

FIGURE 4